PW1 gene/paternally expressed gene 3 (PW1/Peg3) identifies multiple adult stem and progenitor cell populations

Vanessa Besson[a], Piera Smeriglio[a,b], Amélie Wegener[c], Frédéric Relaix[a,d], Brahim Nait Oumesmar[c,e], David A. Sassoon[a,1], and Giovanna Marazzi[a,1]

[a]Myology Group (Stem Cell and Muscle Biology), [d]Myology Group (Mouse Molecular Genetics Group), Unité Mixte de Recherche-S787 Institut National de la Santé et de la Recherche Médicale, University of Pierre and Marie Curie Paris VI, Paris 75634, France; [b]Department of Histology and Medical Embryology, University of Rome "La Sapienza", 00161 Rome, Italy; [c]Le Centre de Recherche de l'Institut du Cerveau et de la Moelle Épinière, Institut National de la Santé et de la Recherche Médicale U975, University of Pierre and Marie Curie Unité Mixte de Recherche-S975, Centre National de la Recherche Scientifique Unité Mixte de Recherche 7225, Paris 75634, France; and [e]Assistance Publique-Hôpitaux de Paris, Groupe hospitalier Pitié-Salpêtrière, Service d'Anatomopathologie Neurologique, Paris 75634, France

Edited* by Eric N. Olson, University of Texas Southwestern, Dallas, TX, and approved May 12, 2011 (received for review March 11, 2011)

A variety of markers are invaluable for identifying and purifying stem/progenitor cells. Here we report the generation of a murine reporter line driven by *Pw1* that reveals cycling and quiescent progenitor/stem cells in all adult tissues thus far examined, including the intestine, blood, testis, central nervous system, bone, skeletal muscle, and skin. Neurospheres generated from the adult PW1-reporter mouse show near 100% reporter-gene expression following a single passage. Furthermore, epidermal stem cells can be purified solely on the basis of reporter-gene expression. These cells are clonogenic, repopulate the epidermal stem-cell niches, and give rise to new hair follicles. Finally, we demonstrate that only PW1 reporter-expressing epidermal cells give rise to follicles that are capable of self-renewal following injury. Our data demonstrate that PW1 serves as an invaluable marker for competent self-renewing stem cells in a wide array of adult tissues, and the PW1-reporter mouse serves as a tool for rapid stem cell isolation and characterization.

bulge | subgranular zone | subventricular zone | crypt | regeneration

Adult stem cells can be proliferative, such as the gut, or quiescent unless activated for tissue repair, as found in muscle (1, 2). In addition to different cell cycle behaviors, adult stem cells are found in anatomically discrete structures or dispersed throughout the tissue with no discernable niche. Finally, certain tissues show remarkable regenerative capacities, whereas others fail to regenerate in response to injury. A variety of markers are invaluable for identifying adult stem cells. Notably, the leucine-rich repeat-containing G protein-coupled receptor 5 (Lgr5), by virtue of a knock-in mouse model, allows for adult stem cell identification and purification from several tissues, although this marker is found primarily with cycling stem cells (3, 4). We identified PW1 in a screen for putative regulators of early skeletal muscle stem cells (5), which was also identified as Peg3 [Paternally expressed gene 3 (6)]. PW1 expression initiates upon gastrulation and remains strongly expressed until birth (5). In postnatal skeletal muscle, PW1 expression is restricted to resident stem cells (satellite cells) as well as $PW1^+$ interstitial cells (PICs) that constitute a second population of postnatal resident skeletal muscle stem cells (7, 8). PW1 regulates two key cell-stress pathways via interaction with the TNF receptor-associated factor 2, as well as the p53-mediated cell death and growth arrest through direct interactions with the Seven in absentia homolog 1 (Siah1) and Bcl2-associated X (Bax) proteins (9, 10). Consistent with these observations, we found that PW1 is required for both TNF and DNA damage/p53-mediated effects on the differentiation of myoblasts (11).

We generated a transgenic PW1-reporter mouse using BAC recombineering. As expected, PW1 protein expression and reporter activity colocalized to satellite cells and PICs in postnatal and adult skeletal muscle. Furthermore, reporter activity and PW1 protein were expressed in a wider range of adult tissues than expected, however, were restricted to cycling and quiescent progenitor/stem cells. Skin cells purified using reporter gene expression are clonogenic, repopulate the epidermal stem cell niches, and give rise to new hair follicles that are capable of self-renewal upon injury.

Results

Generation and Characterization of a Transgenic PW1-Reporter Mouse. We generated the PW1-reporter mouse by placing an internal ribosome entry site (IRES) fused with a nuclear operon lactose gene (*nLacZ*) into exon 9 of the *Pw1* locus using BAC recombineering (Fig. 1*A*). Three founders were generated displaying normal development and similar expression profiles (Fig. S1*A*). One founder was chosen for further analyses. We confirmed a single BAC insertion by FISH (Fig. S1*B*). Reporter activity, mRNA expression, and PW1 protein were coexpressed in the developing limbs, heart, somites, and splanchnic mesoderm, as well the floor and roof plates of the neural tube (Fig. 1 *B–E*), consistent with previous analyses (5). In skeletal muscle we observed ~98% coexpression of reporter activity with endogenous PW1 protein in satellite cells and PICs, as expected (7), whereas myonuclei are not labeled (Fig. 1 *F* and *G*, and Fig. S1*C*), confirming that the BAC transgene contains the essential *cis*-sequences to direct expression to skeletal muscle stem cells.

Reporter Activity and PW1 Expression Identify Stem/Progenitor Cells in a Wide Array of Adult Tissues. Further analyses of this transgenic line revealed a wide range of reporter activity that was restricted to a small number of cells in each tissue examined. Specifically, we detected reporter activity and PW1 protein expression in cells located at the base of the crypt of the small intestine, whereas the differentiated cells along the *villus* axis had no detectable expression (Fig. 2*A*). Intestinal stem cells can be identified as elongated, cycling cells distributed in the 0 to 4 position of the crypt (12–15). As shown in Fig. 2*B*, reporter and PW1-positive cells are intercalated with unlabeled cells in the 0 to 4 position and identical to the distribution reported for Lgr5, which identifies intestinal stem cells (3). We noted that reporter activity and endogenous PW1 expression were not detected

Author contributions: V.B., D.A.S., and G.M. designed research; V.B., P.S., A.W., and G.M. performed research; V.B., F.R., B.N.O., and G.M. contributed new reagents/analytic tools; V.B., P.S., A.W., B.N.O., D.A.S., and G.M. analyzed data; and V.B., D.A.S., and G.M. wrote the paper.

Conflict of interest statement: A patent has been filed for the Tg($Pw1^{IRESnLacZ}$) mouse model. This mouse will be freely made available to any and all academic laboratories for noncommercial use.

*This Direct Submission article had a prearranged editor.

Freely available online through the PNAS open access option.

[1]To whom correspondences may be addressed. E-mail: david.a.sassoon@gmail.com or giovanna.em.marazzi@gmail.com.

This article contains supporting information online at www.pnas.org/lookup/suppl/doi:10.1073/pnas.1103873108/-/DCSupplemental.

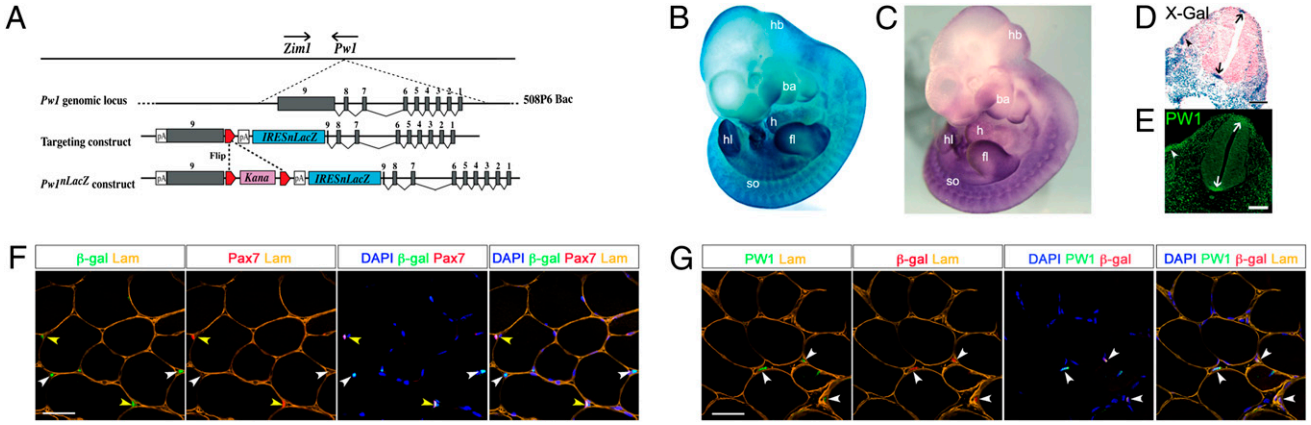

Fig. 1. Generation and characterization of Tg(*Pw1*^{IRESnLacZ}) reporter mice. (*A*) The 508P6 BAC (180 kb) contains all nine exons (gray boxes) of *Pw1*. *Zim1* is located <40 kb from *Pw1* and transcribed in the opposite direction (arrows). An *IRESnLacZ-pA* (blue) and a floxed (red triangles) *kanamycin* (*Kana*, pink) cassette were introduced into the 5′ portion of *Pw1* exon 9. The kanamycin cassette was excised before BAC injection. (*B* and *C*) Whole-mount X-galactosidase (X-Gal) staining of E11 Tg(*Pw1*^{IRESnLacZ}) (*B*) and whole-mount in situ hybridization of E11 wild-type embryos (*C*). The same expression pattern is seen in the hindbrain (hb), brachial arches (ba), heart (h), apical epidermal region of the fore- (fl), and hindlimb (hl) buds, and somites (so). (*D* and *E*) sagittal sections of Tg(*Pw1*^{IRESnLacZ}) (*D*) and wild-type (*E*) embryos at E11. Reporter activity (*D*) and endogenous PW1 protein (*E*) are detected in the floor and roof plate of the neural tube (arrows) and the hypaxial domain of the somites (arrowhead). (*F* and *G*) Cross sections of *Tibialis Anterior* muscle from 7 wk-old reporter mice. Reporter activity is detected in satellite cells (yellow arrowheads), identified by Pax7 expression, and PICs (white arrowheads) (*F*). PW1 and reporter activity colocalize (*G*, white arrowheads). [Scale bars, 100 μm (*D*, *E*), 50 μm (*F*, *G*).]

in the transit amplifying cells cells located in the 5 to 15 position (Fig. 2*B*) (3, 12). Moreover, PW1-reporter activity colocalized with phospho-histone H3 expression that labels actively cycling cells in the crypt consistent with stem cell identity (Fig. 2*C*) (3, 16, 17).

In the testis, reporter activity and endogenous PW1 protein were detected in 7.4% ± 0.4 of the cells located near the basement membrane of all seminiferous tubules (Fig. S2 *A–C* and *F*), consistent with the percentage (18) and location (19) reported for undifferentiated spermatogonia. In contrast to the intestine, testis stem cells are quiescent and we confirmed that reporter expression did not overlap with Ki67 nor phospho-histone H3 (Fig. S2*D*). Testis stem cells express Bmi and GFRA1 (glial cell line-derived neurotrophic factor receptor-α1) (20–22), and we observed ∼16% of reporter-positive cells were positive for Bmi1 expression (Fig. S2 *E* and *F*) (22). In addition, there was near complete overlap with GFRA1 expression (Fig. S2*G*), confirming identity as undifferentiated spermatogonia (20, 21). We extended our analyses to bone, in which reporter activity displayed significant overlap with the runt-related transcription factor 2 (Runx2) (82.2% ± 0.9) and the SRY-box containing gene 9 (Sox9) (83.3% ± 1.6), which are markers for osteo- and chondrogenic progenitors, respectively (23) (Fig. S2 *H–J*). Again, PW1 protein and reporter activity showed complete overlap (Fig. S2*H*).

Our results obtained from muscle, gut, testis, and bone suggested that PW1-reporter activity identifies adult stem/progenitor cells in many tissues. We extended our analyses to the adult CNS, where we detected reporter activity in the subventricular (SVZ) and subgranular zones (SGZ), the CNS stem-cell niches (24, 25) (Fig. 2 *E–G*). The SVZ consists of type B neural stem cells that express GFAP (26). B cells give rise to transit amplifying type C cells that express the oligodendrocyte transcription factor 2 (OLIG2), distal-less homeobox 2 (DLX2), and the murine achaete-scute complex-like 1 (MASH1) (27), and progress to neuroblasts (24) (type A cells) that express doublecortin (28) (DCX) (Fig. 2*D*). In the SVZ, B cells (GFAP$^+$) displayed the highest level of reporter activity (87.9% ± 2.4) (Fig. 2 *E* and *F*). Furthermore, we found that 59.6% ± 11.3 of the reporter cells are label-retaining cells (29). Reduced reporter activity was detected in type C (23.77% ± 2.5) and type A (16.31% ± 3) cells (Fig. 2 *E* and *F*). A similar distribution of labeling was observed in the SGZ (30), in which ∼80% GFAP$^+$ cells displayed reporter activity. As seen for other tissues, reporter activity reflects endogenous PW1 protein expression (92.7% ± 0.2) in neural stem cell niches (Fig. 2*G*), whereas near undetectable levels of PW1 protein were found in differentiated neurons (Fig. 2*H*). It has been demonstrated that neural stem/progenitor cells can be amplified as neurospheres and passaged, leading to an enrichment of type B cells (31); therefore, we generated neurospheres from SVZs isolated from adult reporter mice. We found that cells with high reporter activity increased with subsequent passages (Fig. 2*I*), consistent with the notion that reporter activity is restricted to cells capable of self-renewal (31). Furthermore, endogenous PW1 protein and reporter activity were coexpressed with nestin, a marker of neural stem cells in vitro (Fig. 2*J*). We conclude that PW1/reporter activity identifies stem/progenitor cells of the adult CNS and can be used to track a self-renewing population.

Histological analysis of adult transgenic bone marrow, which contains hematopoietic stem cells, revealed ∼0.72% of labeled cells (Fig. S3*A*). We tested if reporter gene activity could be tracked using a fluorescent substrate for β-galactosidase (β-gal) activity (fluorescein di-β-D-galactopyranoside, FDG). We determined the distribution of reporter expression in the hematopoietic stem cell populations (HSCs) separated on the basis of Lin, CD34, cKit, and Sca1 expression (32) (Fig. 3*A* and Fig. S3*B*). Multipotent long-term HSCs (LT-HSC) self-renew and maintain lifelong production of blood cells and give rise to short-term HSCs (ST-HSC) (33). ST-HSCs retain more limited self-renewal capacity and progress to multipotent progenitors (MPP) that lack self-renewal capacity (Fig. 3*A*) (33). MPPs differentiate into two lineage-restricted progenitors: the common lymphoid- (CLP) and myeloerythroid progenitors. Using FACs analysis, we observed the highest levels of reporter activity in the LT- and ST-HSC populations and progressively lower levels in the more committed MPP and CLP cells (Fig. 3 *B* and *C*). These results were confirmed by direct β-gal immunostaining for each population, which showed complete overlap with endogenous PW1 expression (Fig. 3 *C* and *D*).

Reporter Activity Is Sufficient to Identify a Self-Renewing Population of Epidermal Stem Cells. PW1 protein and reporter activity were detected in the bulge, hair germ, and dermal papilla at all phases of the hair cycle (Fig. 4 *A* and *B*, and Fig. S4 *A–C*, *F*, and *G–J*) corresponding to identified skin stem-cell niches (34–39). Reporter activity colocalized to bulge stem-cell markers cytokeratin 5 (K5), cytokeratin 15 (K15), and CD34 (37, 40, 41) (Fig. S4 *A*, *A′*, *G*, and *H*).

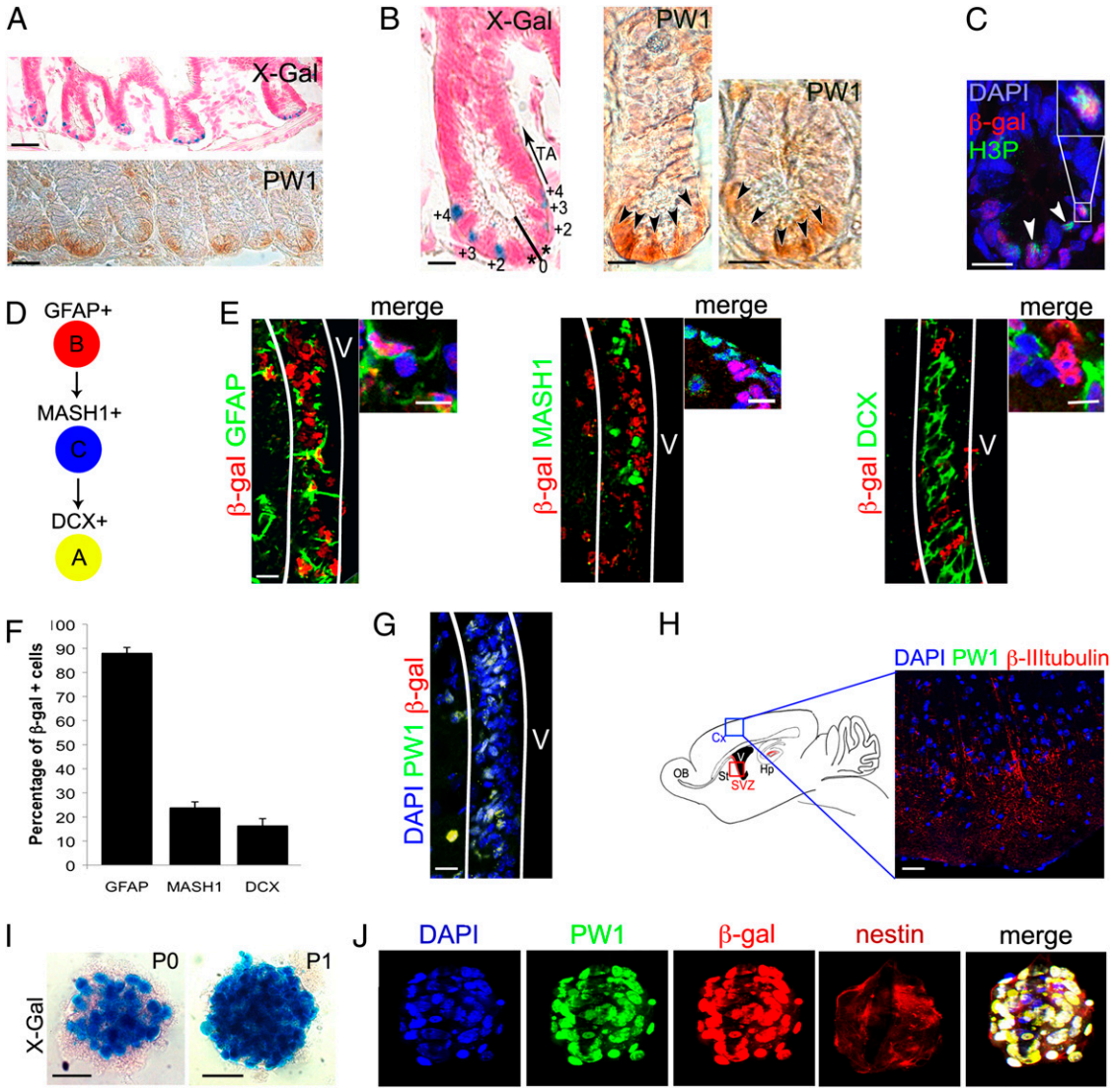

Fig. 2. Reporter activity and PW1 expression identify stem/progenitor cells in the adult small intestine and the CNS. (*A–C*) Representative cross sections of small intestine from 7-wk-old reporter mouse (*A Upper*, *B Left*, and *C*) and wild-type mice (*A Lower*, *B Center* and *Right*) at low (*A*) and high (*B* and *C*) magnification. Histochemical (X-Gal, *A* and *B*) and immunocytochemical (PW1, *A* and *B*) labeling show that reporter activity and endogenous PW1 protein expression are restricted to the basal crypt. We note that the level of PW1 expression in the crypt cells is weak and diffuse. The cells in the crypt are numbered (0 to +4) and the positions of the transit-amplifying cells are indicated (TA, arrow) (*B*). (*C*) Immunofluorescent staining for β-gal and phospho-histone3 (H3P) protein reveals reporter activity in cycling cells (arrowheads). (*Inset*) Double-positive cell at high magnification. (*D*) Summary schema of the adult stem cell lineage in the brain: the B cells (GFAP$^+$) give rise to the transit-amplifying type C cells (MASH1$^+$) and then to the neuroblasts that express doublecortin (DCX, type A). (*E–H*) Identification of the cells expressing the reporter gene and PW1 in the brain. (*E*) Colocalization of β-gal (red) and GFAP, MASH1, and DCX (green), in sagittal sections of the subventricular zone (SVZ, white lines) from a 3-mo-old reporter mouse. Cells at higher magnification are shown on the right. (*F*) Schematic representation of the percentages of β-gal$^+$ cells in each neural stem/progenitor population. Approximately 90% of the GFAP$^+$ neuronal stem cells express β-gal. The percentage of β-gal$^+$ cells sharply decreases in the more committed (MASH$^+$ and DCX$^+$) progenitor populations. Values represent mean % ± SEM. (*G*) Colocalization of reporter (β-gal) and PW1 in the SVZ (white lines) V: ventricle. (*H*) (*Right*) Schematic representation of the brain showing the area of cortex (Cx, blue rectangle) corresponding to the photomicrograph shown in the left. (*Left*) Sagittal cryosection of 3-mo-old reporter mouse brain stained for PW1 and β-III-tubulin. PW1 is not detected in differentiated neurons identified by β-III-tubulin expression. Hp, hippocampus; OB, olfactory bulb; St, striatum; SVZ, red rectangle, subventricular zone. (*I*) X-Gal coloration staining of neurospheres, generated from the SVZ of 2-mo-old reporter mice before (P0) and after (P1) one passage. The number of β-gal$^+$ cells by neurosphere increases after one passage (P1). (*J*) Colocalization of PW1 (green) and β-gal (red) in nestin-positive neurospheres after one passage. [Scale bars, 20 μm (*I*), 30 μm (*E*, *G* and *H*), 50 μm (*B* and *C*), 150 μm (*A*).]

We noted reporter expression in the hair germ stem cells, which were positive for K15 and P-Cadherin (36, 37, 40) (Fig. S4 *A′* and *B*). The dermal papilla cells were identified by vimentin staining (35, 36, 42) (Fig. S4 *I* and *J*). We observed that reporter activity and PW1 protein were not detected in the interfollicular epidermis nor in differentiated cellular compartments using markers of the outer root sheath (AE15) (43), the inner root sheath, the bulb (CCAAT displacement protein) (44), and the companion layer (K6) (45) (Fig. S4 *C–E* and *F′*). Reporter and endogenous PW1 protein expression overlapped. We isolated epidermal cells from the back skin of PW1-reporter mice crossed to *H2B-EGFP* mice (expressing ubiquitous GFP under the *histone2B* promoter) to follow engrafted cell fates. To eliminate contamination between β-gal$^+$ and β-gal$^-$ populations, we used stringent FACs parameters and verified purity by direct immunostaining of the fractions (Fig. 4*C* and Fig. S4*K*). Under these conditions, the β-gal$^+$ fraction represented ~0.6% of the epidermal cell preparation and displayed ~98% (98.4% ± 1.2) coexpression with PW1 (Fig. 4 *C* and *D*). In culture,

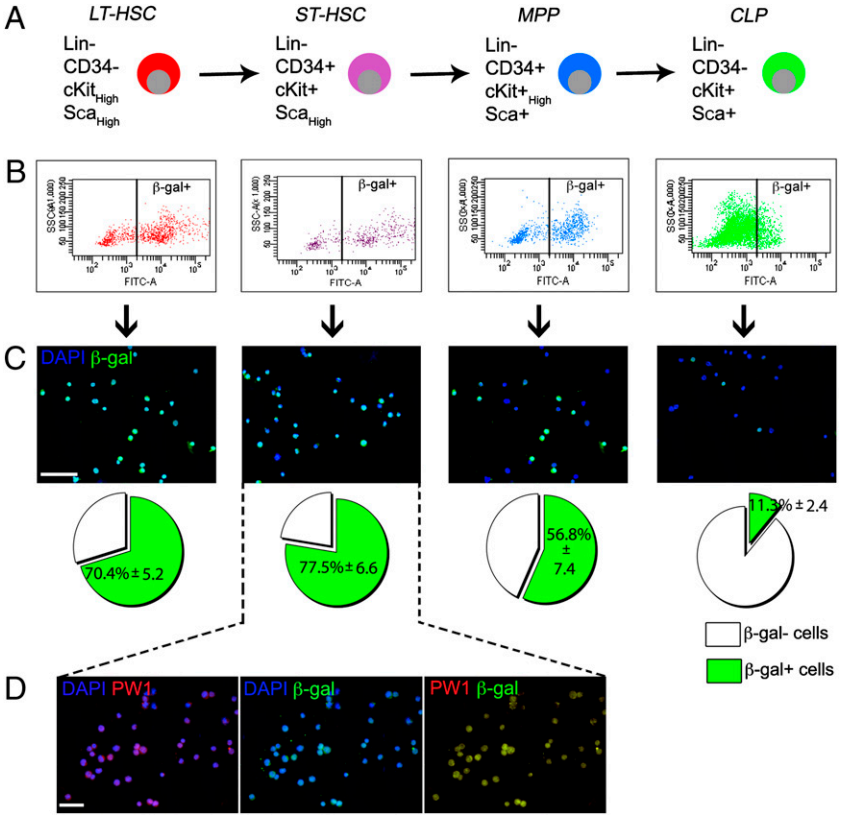

Fig. 3. Reporter activity is highest in the primitive hematopoietic stem cell populations from 7-wk-old reporter mice. (*A*) Four populations were obtained based on cell surface gene expression profiles: LT-HSC and ST-HSC, MPP, and CLP. (*B* and *C*) Each population was sorted based on β-gal expression (*B*). Reporter expression was confirmed by immunofluorescence (*C*) and the percentage of β-gal$^+$ cells was counted for each populations (*C*, *Lower*). Reporter activity is higher in the stem cell populations and decreases in the progenitors. Values represent mean % ± SEM. (*D*) Immunostaining for PW1 and β-gal in the purified ST-HSC population shows a complete colocalization. [Scale bars, 50 μm (*C* and *D*).]

the β-gal$^+$ cells displayed a high level of clonogenicity (47.3 colonies ± 1.6) compared with the β-gal$^-$ cells (12.7 colonies ± 1.1) (Fig. 4 *E* and *F*). We further engrafted both populations to test their stem cell capacity in vivo. We observed robust contribution of β-gal$^+$ cells (31.6% ± 2.4) to the hair follicles compared with poor contribution by the β-gal$^-$ population (5.8% ± 0.4) 3 wk following engraftment (Fig. 4 *G–J*). Following injection of the β-gal$^+$/GFP$^+$ cells, we observed that GFP-labeled cells no longer expressed β-gal in the differentiated hair follicles, sebaceous glands, and the interfollicular epidermis, as shown by Keratin 14 (K14) coexpression (Fig. S4 *L–N*), demonstrating that β-gal$^+$ cells are competent progenitors capable of reconstituting hair follicles. Furthermore, we observed GFP$^+$/β-gal$^+$ cells restricted to the bulge and dermal papilla of the hair follicles (Fig. 4 *K–Q*), demonstrating that β-gal$^+$ cells can reconstitute their niche and that reporter gene expression remained restricted to stem cells following engraftment. Although these observations are consistent with a stem cell identity for reporter-expressing cells, a critical feature of stem cells is their capacity to undergo self-renewal. Therefore, we tested the self-renewal capacity of the engrafted cells by depilating the grafts (Fig. 4 *R–U*) 1 mo following engraftment. We observed that β-gal$^+$ cell-derived grafts showed robust regrowth (Fig. 4 *R* and *S*), whereas grafts resulting from β-gal$^-$ cells displayed poor initial hair growth (Fig. 4 *I*, *J*, and *T*) and almost no regeneration following depilation (Fig. 4*U*). Our results demonstrate that the β-gal$^+$ cells give rise to differentiated epidermal cell fates, reconstitute their niche, and self-renew.

Discussion

We initially isolated PW1 in a screen designed to identify early stem cells in the skeletal muscle lineage (5). Our previous characterization of PW1 in postnatal skeletal muscle revealed expression in satellite cells that have long been accepted as the major resident progenitor cell (8); however, we also observed PW1 expression in a subpopulation of interstitial cells. Detailed analyses of the PICs demonstrated that they are a distinct population that can generate new myofibers following engraftment into damaged muscle (7). Moreover, whereas both satellite cells and PICs give rise to muscle and satellite cells, only PICs give rise to PICs, fulfilling a key criteria of a stem cell, including the ability to self renew (7). Whereas muscle stem cells remain quiescent and blood stem cells proliferate slowly, intestinal stem cells divide continuously to generate the steady turnover of intestinal *villi* (3). These cells were characterized using the Lgr5 knock-in mouse that identifies a cell population with specific cellular positions in the crypt that are positive for markers of cell proliferation (3, 17). We show here that PW1 and reporter expression overlap completely with these multiple lineages of stem cells. Although we initially discovered that PW1 identified a unique muscle stem-cell population, combined with data presented here, our results reveal that PW1 can be used to identify many lineages of adult stem cells in situ.

For each lineage examined in this study, we found that cells that expressed PW1 also expressed tissue-specific stem-cell markers. We therefore tested whether the expression of PW1 can be used to track stem cells once isolated from the tissue. Stem cells from the CNS can be isolated and expanded in vitro by generating neurospheres (31). When single cells are obtained from the stem-cell niches of the CNS, neural stem cells are grown under suspension and after one passage, neurospheres contain mostly early neural stem cells (46) that express PW1 protein and reporter activity, as well as neural stem-cell markers revealing that PW1 expression is a marker for stem cells in vitro as well as in vivo.

We wished to test the utility of the PW1 reporter for a single-step isolation of stem cells from the skin. We show here that PW1 reporter-expressing epidermal cells are capable of reconstituting hair follicles when engrafted into nude mice. When the grafts are challenged to regenerate, we found that only grafts obtained from PW1-expressing cells were capable of robust regeneration. Coupled with our observations using lineage tracing of double-labeled PW1-expressing cells (expressing nuclear GFP) in which we demonstrate that PW1$^+$ cells also repopulate the hair follicle stem cell niches, we conclude that PW1 marks the self-renewing stem-cell population in

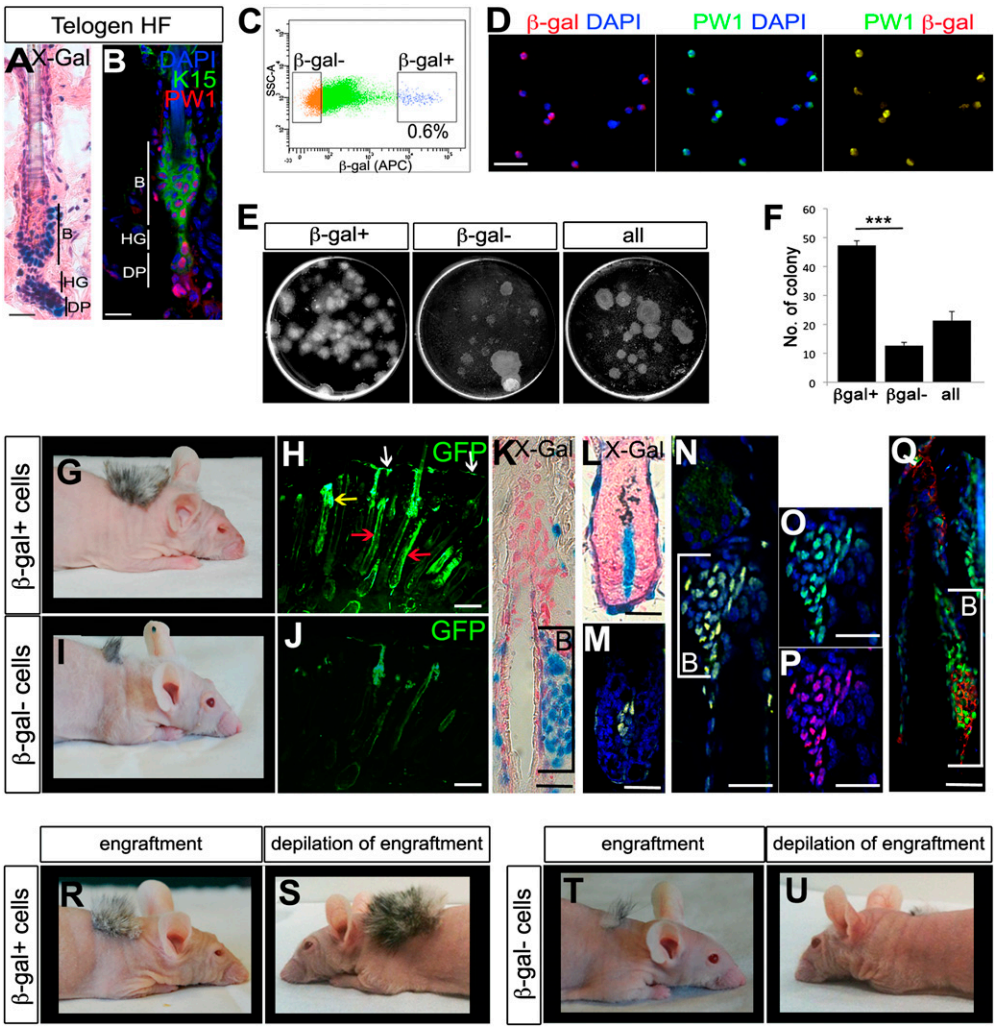

Fig. 4. PW1$^+$ cell population corresponds to competent and self-renewing hair-follicle stem cells. (*A*) Histochemical staining of longitudinal sections of 7-wk-old reporter mice hair follicle (HF) in telogen. Reporter activity is detected in the stem cells compartment of the skin. B, bulge; DP, dermal papilla; HG, hair germ. (*B*) Representative longitudinal section of 7-wk-old wild-type mouse hair follicle (HF) in telogen stained for PW1 (red) and K15 (green) to identify the bulge (B). As in the case of the reporter, PW1 expression is restricted to the bulge (B), hair germ (HG), and dermal papilla (DP). (*C*) Single-cell preparations from adult (7-wk-old) *H2B-EGFP* × Tg (*Pw1*^{IRESnLacZ}) mouse epidermis were FACS-sorted on the basis of β-gal expression. Approximately 0.6% of sorted cells are β-gal$^+$. (*D*) β-Gal and PW1 in freshly sorted β-gal$^+$ cells. (*E*) Sorted (β-gal$^+$, β-gal$^-$) and unsorted (all) cells were plated for clonogenicity experiment and colonies were stained with Rhodamine after 16 d in culture. (*F*) Schematic representation of the number of colonies formed by β-gal$^+$, β-gal$^-$, and unsorted (all) cells as shown in *E* per dish. β-Gal$^+$ cells form more colonies compared with β-gal$^-$ and unsorted cells. Values represent β-gal number of colony ± SEM *t* test (***$P < 0.001$). (*G* and *I*) Hair growth resulting from β-gal β-gal$^+$ versus β-gal$^-$ cell grafts in 2-mo-old nude mice. (*H* and *J*) Micrographs of graft tissue sections showing GFP expression in the epidermis (white arrow), sebaceous gland (yellow arrow), and hair follicle (red arrows). (*K*–*Q*) Photomicrographs showing the bulge (B, brackets; *K* and *N*–*Q*) and dermal papilla (*L* and *M*). Longitudinal sections are stained either histochemically (X-Gal) (*K* and *L*) or by immunofluorescence for β-gal (*M*, *N*, and *P*), GFP (*M*–*O* and *Q*, green) and K15 (*Q*, red). *M* and *N* are merged images. (*R*–*U*) Photographs show the hair growth of β-gal$^+$ (*R* and *S*) versus β-gal$^-$ (*T* and *U*) cell grafts before (*R* and *T*) and after injury (depilation, *S* and *U*). [Scale bars, 10 μm (*A* and *B*), 30 μm (*D*), 5 μm (*H* and *J*), 50 μm (*K*–*Q*).]

the skin. As seen with neurospheres, these cells maintain reporter-gene expression in vitro, demonstrating an application for this mouse model as a means to select and subsequently screen stem cells for conditions that support stem cell expansion in culture. Presently we are extending our analyses to a wide array of adult tissues in which the stem-cell niche has not been well characterized. As such, this mouse model promises applications for both basic stem cell biology and regenerative medicine.

Materials and Methods

Generation of Tg(*Pw1*^{IRESnLacZ}) Mice. All work with mice was carried out in adherence to French Government and European guidelines and was approved by the Pierre et Marie Curie University. Transgenic mice were generated using BAC recombineering, as previously described (47). The *Pw1*-containing BAC clone (ID#508P6, 180 kb) comes from a 129Sv library. An *IRESnLacZ* (3.8 kb) cassette, a SV40 polyadenylation signal, and a *kanamycin* selection gene floxed by two FLP recognition target sites (1 kb) were introduced into the 5′ portion of *Pw1* exon 9 (+19,302 bp, Acc:MGI:104748; NCBIM37). The kanamycin cassette was excised by arabinose treatment. The transgenic BAC allele was injected into oocytes to generate founders that were identified by PCR and maintained in a C57BL6/J background. The resulting reporter mouse is called B6-Tg(*Pw1*^{IRESnLacZ})26sas.

Histological Analyses. Whole-mount in situ hybridization was performed as previously described (48) with a *Pw1* riboprobe (865 bp) generated from the PstI digestion of exon 9 cDNA.

Three independent BrdU-labeled retaining experiments were performed, as previously described (29).

Tibialis anterior muscles were snap frozen in liquid nitrogen-cooled isopentane; bones were treated with a 5.5% EDTA (10% Formalin) solution before freezing in liquid nitrogen. Testis were embedded in paraffin. All other tissues were fixed in 4% paraformaldehyde, embedded in 15% sucrose, and frozen in liquid nitrogen. Cryosections (5–8 μm) and cytospin preparations were fixed 15 min at room temperature with 4% PFA before X-Gal staining (49) for 3 to 5 h or processed for immunofluorescence or immunocytochemistry, as previously described (8, 11, 50). For primary antibodies and secondary antibodies, see *SI Materials and Methods*. Qualitative and quantitative analyses were performed from at least three independent experiments. FISH was performed as previously described (51) with a 180-kb BAC (ID#508P6) probe covering the *Pw1* gene.

FACS Analysis. Single-cell preparations were obtained from back skin by enzymatic digestion (trypsin; Invitrogen) overnight at 4 °C to separate the epidermis from the dermis (52).

Epidermal cell preparations (4) or bone marrow of 7-wk-old Tg(*Pw1*^{IRESnLacZ}) mice were stained with 10 ng/mL of appropriate antibodies (see *SI Materials and Methods*) and sorted by using a FACSAria (Becton Dickinson). To detect nuclear β-gal activity, FDG (53) staining kits (Molecular Probes) were used according to the manufacturer's instructions. β-Gal$^+$ cells were defined as having a signal higher than the cells isolated from non transgenic mouse.

Transplantation. Five independent transplantations (5 × 10^5 cells) were performed as described (54). Freshly sorted cells were immediately frozen,

pooled, and engrafted between the epidermis and the dermis of a newborn skin before grafting on recipient nude mice. Cell contribution was determined by counting the percentage of GFP$^+$ follicles. Four weeks after engraftment, the engrafted area of two reporter mice per group were injured by depilation and hair regrowth was evaluated 4 wk later.

Clonogenicity Assay. 2Four independent colony-forming assays were performed as described previously (4). Three-thousand freshly sorted (β-gal$^+$, β-gal$^-$) or unsorted cells (all) were plated and colonies were stained with 1% Rhodamine B after 16-d culture and counted. Qualitative and quantitative analyses were performed from at least three independent experiments. Statistical analyses were done using the Student *t* test.

Neurospheres. SVZ cells were collected from five adult (2-mo-old) reporter mice and seeded at 10,000 cells/cm^2 (55). Neurospheres were grown in floating cultures as described previously (31). The neurospheres were passaged every 4 wk. Two independent experiments were performed.

ACKNOWLEDGMENTS. We thank K. Bismuth and Y. Barrandon for helpful discussion and assistance, C. Blanc and B. Hoareau for FACS assistance, F. Langa for transgenic service, and B. Keren for the FISH analyses. This work was supported by a grant from the French Ministry of Research "Chaire d'Excellence," the Muscular Dystrophy Association of America (to D.A.S.); grants from the French Foundation (Fondation pour l'Aide á la Recherche sur la Sclérose en Plaques) and the National Multiple Sclerosis Society (to B.N.O); Institut National de la Santé et de la Recherche Médicale Avenir, Decrypthon, Ligue Nationale Contre le Cancer funding and Institut National du Cancer/Canceropole research grant programs (F.R.); A.W. is a recipient of fellowship from the French Ministry of Education and Research and P.S. is a recipient of a Ph.D. fellowship Fondazione Pasteur-Cenci Bolognetti. This work received funding from the European Community Seventh Framework Programme projects Optimization of Stem Cell Therapy for Degenerative Epithelial and Muscle Diseases (OPTISTEM) (Health-F5-2009-223098) and ENDOSTEM (Activation of vasculature associated stem cells and muscle stem cells for the repair and maintenance of muscle tissue) (Agreement 241440), and support from the Agence Nationale de la Recherche (ANR-Epistem). The Myology Group is the beneficiary of a Strategic Plan Support from the Association Française contre les Myopathies and is affiliated with the Association Institut Myologie.

1. Fuchs E (2009) The tortoise and the hair: Slow-cycling cells in the stem cell race. *Cell* 137:811–819.
2. Magavi SS, Leavitt BR, Macklis JD (2000) Induction of neurogenesis in the neocortex of adult mice. *Nature* 405:951–955.
3. Barker N, et al. (2007) Identification of stem cells in small intestine and colon by marker gene Lgr5. *Nature* 449:1003–1007.
4. Jaks V, et al. (2008) Lgr5 marks cycling, yet long-lived, hair follicle stem cells. *Nat Genet* 40:1291–1299.
5. Relaix F, et al. (1996) Pw1, a novel zinc finger gene implicated in the myogenic and neuronal lineages. *Dev Biol* 177:383–396.
6. Kuroiwa Y, et al. (1996) Peg3 imprinted gene on proximal chromosome 7 encodes for a zinc finger protein. *Nat Genet* 12:186–190.
7. Mitchell KJ, et al. (2010) Identification and characterization of a non-satellite cell muscle resident progenitor during postnatal development. *Nat Cell Biol* 12:257–266.
8. Nicolas N, Marazzi G, Kelley K, Sassoon D (2005) Embryonic deregulation of muscle stress signaling pathways leads to altered postnatal stem cell behavior and a failure in postnatal muscle growth. *Dev Biol* 281:171–183.
9. Relaix F, et al. (2000) Pw1/Peg3 is a potential cell death mediator and cooperates with Siah1a in p53-mediated apoptosis. *Proc Natl Acad Sci USA* 97:2105–2110.
10. Relaix F, Wei XJ, Wu X, Sassoon DA (1998) Peg3/Pw1 is an imprinted gene involved in the TNF-NFkappaB signal transduction pathway. *Nat Genet* 18:287–291.
11. Schwarzkopf M, Coletti D, Sassoon D, Marazzi G (2006) Muscle cachexia is regulated by a p53-PW1/Peg3-dependent pathway. *Genes Dev* 20:3440–3452.
12. Cheng H, Leblond CP (1974) Origin, differentiation and renewal of the four main epithelial cell types in the mouse small intestine. V. Unitarian theory of the origin of the four epithelial cell types. *Am J Anat* 141:537–561.
13. Bjerknes M, Cheng H (1981) The stem-cell zone of the small intestinal epithelium. III. Evidence from columnar, enteroendocrine, and mucous cells in the adult mouse. *Am J Anat* 160:77–91.
14. Bjerknes M, Cheng H (1999) Clonal analysis of mouse intestinal epithelial progenitors. *Gastroenterology* 116:7–14.
15. Stappenbeck TS, Mills JC, Gordon JI (2003) Molecular features of adult mouse small intestinal epithelial progenitors. *Proc Natl Acad Sci USA* 100:1004–1009.
16. Bradbury EM (1992) Reversible histone modifications and the chromosome cell cycle. *Bioessays* 14:9–16.
17. Hans F, Dimitrov S (2001) Histone H3 phosphorylation and cell division. *Oncogene* 20: 3021–3027.
18. Hobbs RM, Seandel M, Falciatori I, Rafii S, Pandolfi PP (2010) Plzf regulates germline progenitor self-renewal by opposing mTORC1. *Cell* 142:468–479.
19. Takubo K, et al. (2008) Stem cell defects in ATM-deficient undifferentiated spermatogonia through DNA damage-induced cell-cycle arrest. *Cell Stem Cell* 2:170–182.
20. Grisanti L, et al. (2009) Identification of spermatogonial stem cell subsets by morphological analysis and prospective isolation. *Stem Cells* 27:3043–3052.
21. Meng X, et al. (2000) Regulation of cell fate decision of undifferentiated spermatogonia by GDNF. *Science* 287:1489–1493.
22. Zhang S, et al. (2008) Expression localization of Bmi1 in mice testis. *Mol Cell Endocrinol* 287:47–56.
23. Zhou G, et al. (2006) Dominance of SOX9 function over RUNX2 during skeletogenesis. *Proc Natl Acad Sci USA* 103:19004–19009.
24. Doetsch F (2003) A niche for adult neural stem cells. *Curr Opin Genet Dev* 13:543–550.
25. Suh H, Deng W, Gage FH (2009) Signaling in adult neurogenesis. *Annu Rev Cell Dev Biol* 25:253–275.
26. Lois C, Alvarez-Buylla A (1994) Long-distance neuronal migration in the adult mammalian brain. *Science* 264:1145–1148.
27. Parras CM, et al. (2004) Mash1 specifies neurons and oligodendrocytes in the postnatal brain. *EMBO J* 23:4495–4505.
28. Brown JP, et al. (2003) Transient expression of doublecortin during adult neurogenesis. *J Comp Neurol* 467:1–10.
29. Pluchino S, et al. (2008) Persistent inflammation alters the function of the endogenous brain stem cell compartment. *Brain* 131:2564–2578.
30. Seri B, García-Verdugo JM, McEwen BS, Alvarez-Buylla A (2001) Astrocytes give rise to new neurons in the adult mammalian hippocampus. *J Neurosci* 21:7153–7160.
31. Pastrana E, Cheng LC, Doetsch F (2009) Simultaneous prospective purification of adult subventricular zone neural stem cells and their progeny. *Proc Natl Acad Sci USA* 106: 6387–6392.
32. Blank U, Karlsson G, Karlsson S (2008) Signaling pathways governing stem-cell fate. *Blood* 111:492–503.
33. Morrison SJ, Wandycz AM, Hemmati HD, Wright DE, Weissman IL (1997) Identification of a lineage of multipotent hematopoietic progenitors. *Development* 124:1929–1939.
34. Driskell RR, Giangreco A, Jensen KB, Mulder KW, Watt FM (2009) Sox2-positive dermal papilla cells specify hair follicle type in mammalian epidermis. *Development* 136:2815–2823.
35. Fernandes KJ, et al. (2004) A dermal niche for multipotent adult skin-derived precursor cells. *Nat Cell Biol* 6:1082–1093.
36. Greco V, et al. (2009) A two-step mechanism for stem cell activation during hair regeneration. *Cell Stem Cell* 4:155–169.
37. Morris RJ, et al. (2004) Capturing and profiling adult hair follicle stem cells. *Nat Biotechnol* 22:411–417.
38. Taylor G, Lehrer MS, Jensen PJ, Sun TT, Lavker RM (2000) Involvement of follicular stem cells in forming not only the follicle but also the epidermis. *Cell* 102:451–461.
39. Toma JG, et al. (2001) Isolation of multipotent adult stem cells from the dermis of mammalian skin. *Nat Cell Biol* 3:778–784.
40. Trempus CS, et al. (2003) Enrichment for living murine keratinocytes from the hair follicle bulge with the cell surface marker CD34. *J Invest Dermatol* 120:501–511.
41. Chebotaev D, Yemelyanov A, Zhu L, Lavker RM, Budunova I (2007) The tumor suppressor effect of the glucocorticoid receptor in skin is mediated via its effect on follicular epithelial stem cells. *Oncogene* 26:3060–3068.
42. Morris RJ, Potten CS (1999) Highly persistent label-retaining cells in the hair follicles of mice and their fate following induction of anagen. *J Invest Dermatol* 112:470–475.
43. Youssef KK, et al. (2010) Identification of the cell lineage at the origin of basal cell carcinoma. *Nat Cell Biol* 12:299–305.
44. Silva-Vargas V, et al. (2005) Beta-catenin and Hedgehog signal strength can specify number and location of hair follicles in adult epidermis without recruitment of bulge stem cells. *Dev Cell* 9:121–131.
45. Winter H, et al. (1998) A novel human type II cytokeratin, K6hf, specifically expressed in the companion layer of the hair follicle. *J Invest Dermatol* 111:955–962.
46. Reynolds BA, Weiss S (1996) Clonal and population analyses demonstrate that an EGF-responsive mammalian embryonic CNS precursor is a stem cell. *Dev Biol* 175:1–13.
47. Lee EC, et al. (2001) A highly efficient *Escherichia coli*-based chromosome engineering system adapted for recombinogenic targeting and subcloning of BAC DNA. *Genomics* 73:56–65.
48. Tajbakhsh S, Rocancourt D, Cossu G, Buckingham M (1997) Redefining the genetic hierarchies controlling skeletal myogenesis: Pax-3 and Myf-5 act upstream of MyoD. *Cell* 89:127–138.
49. Relaix F, Rocancourt D, Mansouri A, Buckingham M (2004) Divergent functions of murine Pax3 and Pax7 in limb muscle development. *Genes Dev* 18:1088–1105.
50. Coletti D, Yang E, Marazzi G, Sassoon D (2002) TNFalpha inhibits skeletal myogenesis through a PW1-dependent pathway by recruitment of caspase pathways. *EMBO J* 21: 631–642.
51. Bismuth K, et al. (2008) An unstable targeted allele of the mouse *Mitf* gene with a high somatic and germline reversion rate. *Genetics* 178:259–272.
52. Jensen KB, Driskell RR, Watt FM (2010) Assaying proliferation and differentiation capacity of stem cells using disaggregated adult mouse epidermis. *Nat Protoc* 5: 898–911.
53. Fiering SN, et al. (1991) Improved FACS-Gal: Flow cytometric analysis and sorting of viable eukaryotic cells expressing reporter gene constructs. *Cytometry* 12:291–301.
54. Claudinot S, Nicolas M, Oshima H, Rochat A, Barrandon Y (2005) Long-term renewal of hair follicles from clonogenic multipotent stem cells. *Proc Natl Acad Sci USA* 102: 14677–14682.
55. Doetsch F, Petreanu L, Caille I, Garcia-Verdugo JM, Alvarez-Buylla A (2002) EGF converts transit-amplifying neurogenic precursors in the adult brain into multipotent stem cells. *Neuron* 36:1021–1034.